Perovskite Solar Cells Hot Paper

International Edition: DOI: 10.1002/anie.201604399
German Edition: DOI: 10.1002/ange.201604399

Hexaazatrinaphthylene Derivatives: Efficient Electron-Transporting Materials with Tunable Energy Levels for Inverted Perovskite Solar Cells

*Dongbing Zhao[+], Zonglong Zhu[+], Ming-Yu Kuo, Chu-Chen Chueh, and Alex K.-Y. Jen**

Abstract: *Hexaazatrinaphthylene (HATNA) derivatives have been successfully shown to function as efficient electron-transporting materials (ETMs) for perovskite solar cells (PVSCs). The cells demonstrate a superior power conversion efficiency (PCE) of 17.6% with negligible hysteresis. This study provides one of the first nonfullerene small-molecule-based ETMs for high-performance p–i–n PVSCs.*

The rapid progress made in the development of perovskite solar cells (PVSCs) over the last few years has significantly increased their competitiveness with the existing inorganic solar cells made from Si, CdTe, and CIGS (copper, indium, gallium, selenide).[1] The exceptional semiconducting properties of perovskites allow flexibility in fabricating devices using either the conventional n–i–p or the inverted p–i–n configurations with proper charge-transporting materials (p refers to a p-type semiconductor, n to an n-type semiconductor, and i an undoped intrinsic semiconductor in these configurations). In both cases, further improvements in power conversion efficiency (PCE) and current–voltage (J–V) hysteresis can be achieved since the interface loss can be minimized by interface modification.[2] Recently, hole-transporting materials (HTM) have been vigorously developed and have shown great promise in continuously improving device performance and stability.[3] However, the pace of developing suitable electron-transporting materials (ETM) is lagging behind compared to the impressive progress made in developing HTMs. The conventional n–i–p PVSCs primarily employ transition-metal oxides (TMOs) as the ETM, which usually require high temperatures and sophisticated preparatory procedures.[4] On the other hand, the choice of ETM for inverted p–i–n PVSCs is often limited by using fullerene and its derivatives.[5,6] Despite the attractive properties offered by fullerenes, their high cost, poor ambient stability, and their monotonous tunability in terms of frontier energy levels are disadvantageous.[7] Therefore, there is an urgent need to develop efficient nonfullerene organic ETMs with tunable energy levels and comparable properties to fullerenes for application in PVSCs. However, it is difficult to find suitable organic ETMs to obtain high-performance PVSCs,[8] partially due to the limited numbers of existing efficient n-type molecular building blocks.

Hexaazatrinaphthylene (HATNA) derivatives have attracted attention as promising ETMs as a result of their low cost, high charge mobility, and large band gap.[9] However, HATNA derivatives have not been used as ETMs for PVSCs to date because of the relatively high LUMO levels of the parent HATNA compared to the conduction band minimum (CBM) of most frequently studied $CH_3NH_3PbI_3$ (denoted $MAPbI_3$; Figure 1a). Marder et al. and Selzer and co-workers previously demonstrated that HATNA-F_6 possesses a comparable energy level and optical band gap (E_g^{opt}) with fullerene (electron affinity EA = 4.2 eV, ionization potential IP = 7.70 eV, E_g^{opt} = 2.9 eV; Figure 1a).[10] The sufficiently high electron mobility and low extinction coefficient in visible light of HATNA-F_6 could be ideal for the development of highly efficient HATNA-F_6-based ETMs for application in PVSCs (Figure 1a).[10] However, there are several challenges that need to be overcome before they can be accessed as ETMs for PVSCs, such as the difficulty to modify highly crystalline HATNA-F_6 and its poor solution processability.

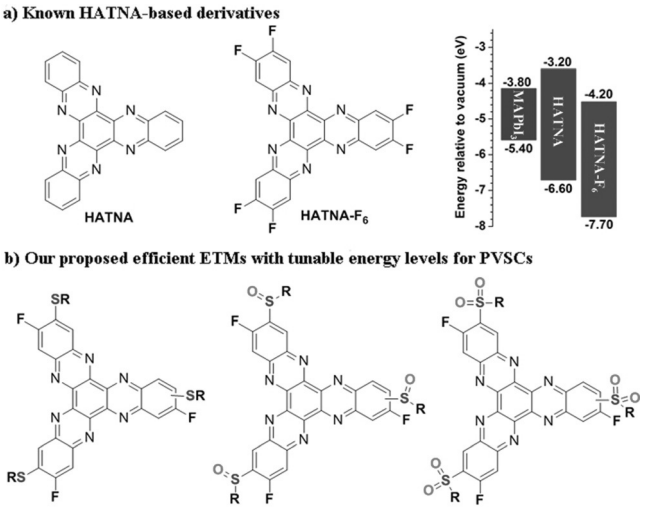

Figure 1. Previously reported HATNA derivatives and new structures reported herein.

Herein, we present a design strategy for a HATNA-based ETM involving the replacement of three F groups on the HATNA-F_6 core with three alkylsulfanyl chains bearing different alkyl-chain lengths (Figure 1b). This modification

[*] Dr. D. Zhao,[+] Dr. Z. Zhu,[+] Prof. Dr. M.-Y. Kuo, Dr. C.-C. Chueh, Prof. Dr. A. K.-Y. Jen
Department of Materials Science and Engineering
University of Washington
Seattle, WA 98195 (USA)
E-mail: ajen@u.washington.edu

[+] These authors contributed equally to this work.

Supporting information for this article can be found under: http://dx.doi.org/10.1002/anie.201604399.

should improve the solubility of the compound in organic solvents[11] and allow the molecule to potentially passivate the surface traps of perovskite.[12] However, the introduction of alkylsulfanyl chains will raise the LUMO level significantly and lead to strong intramolecular charge transfer (ICT) induced absorption, which may be unfavorable for the devices. To ensure the LUMO can be aligned properly with the CBM of $MAPbI_3$ and to decrease the parasitic absorption, we also prepared molecules with different oxidation states for the sulfur atoms in the alkylsulfanyl chains, varying the nature of the sulfur species from sulfide (S), to sulfoxide (SO), to sulfone (SO_2; Figure 1b). As a result, PVSCs fabricated with the p–i–n architecture using a HATNA-F_3-derived ETM showed an encouraging PCE of 17.6% with negligible hysteresis. This constitutes one of the first examples using a nonfullerene organic ETM in which a comparable performance is achieved to those of PCBM-based p–i–n PVSCs (PCBM = phenyl-C61-butyric acid methyl ester).

In our initial experiment, HATNA-F_6 was treated with K_2CO_3 and 3 equiv of 1-butanethiol in DMF at 100 °C for 24 h, in an attempt to induce the functionalization of butyl sulfide through nucleophilic substitution. Unfortunately, only a small amount of the desired product could be obtained, and mostly side products and starting materials were recovered. To address this, the synthetic route was switched to a stepwise reaction (see Scheme S1 in the Supporting Information). 4,5-Difluoro-2-nitroaniline S1 was first reacted with 1-butanethiol and 1-heptanethiol through nucleophilic substitution to obtain the alkylsulfanyl-substituted derivatives S2 and S3, respectively, which were then reduced by $SnCl_2$ to form the corresponding diamines S4 and S5. Finally, thioalkyl-substituted hexaazatrinaphthylene derivatives with different alkyl chain lengths (HATNAS3C4 and HATNAS3C7; Scheme 1) were synthesized by condensing diamines S4 and S5 with hexaketocyclohexane octahydrate in the presence of acetic acid. Notably, HATNAS3C4 and HATNAS3C7 were formed as a mixture of C_{3h}- and C_s-symmetric isomers. Unexpectedly, the HATNAS3C7 isomers could be isolated by column chromatography to obtain HATNAS3C7-C_{3h} and HATNAS3C7-C_s. Attempts to separate the isomers of HATNAS3C4 were unsuccessful. Next, the pure product HATNAS3C7-C_s was further oxidized by *m*-chloroperoxybenzoic acid (*m*-CPBA) to produce the corresponding sulfoxide (HATNASOC7-C_s) and sulfone (HATNASO2C7-C_s; see Scheme 1).

To estimate the molecular geometries of these HATNA derivatives, density functional theory (DFT) calculations were performed. As can be seen in Figure S1, all of the molecules have discotic, rigid, and fully conjugated geometries, facilitating face-on π–π stacking which should provide good charge transport in the film state. The optical properties of these materials in solution and in thin films were characterized by UV/Vis absorption spectroscopy (Figure 2a and Figure S3). The corresponding spectroscopic data are summarized in Table S1. Optical absorption spectra of these compounds are in accordance with our hypothesis. The thin films of alkylsulfanyl-substituted HATNA derivatives (HATNAS3C4, HATNAS3C7, HATNAS3C7-C_{3h}, and HATNAS3C7-C_s) all showed strong ICT-based absorption bands centered at $\lambda \approx 453$ nm. Upon application as the ETM for PVSCs, this parasitic ICT absorption may lead to a decrease in photocurrent. Fortunately, switching the sulfide (HATNAS3C7-C_s) to sulfoxide (HATNASOC7-C_s) and sulfone (HATNASO2C7-C_s) resulted in a significantly blue-shifted and decreased ICT absorption band in both the thin film and in solution (Figure 2a). From the thin film absorption onset, the optical band gaps are estimated and listed in Table S1. To investigate the energy levels of these HATNA derivatives, electrochemical cyclic voltammetry (CV) has been employed to measure their redox properties (Figure S4). By calculating from the reductive onset potentials and the optical band gaps, LUMO/HOMO energy levels were derived and are summarized in Table S1. The trend is in agreement with that obtained from DFT calculations (Figure S2). As expected, the energy levels of these HATNA derivatives can be systematically tuned by converting sulfide into sulfoxide and sulfone. The LUMO and HUMO levels of the corresponding sulfoxide (HATNASOC7-C_s) and sulfone (HATNASO2C7-C_s) are

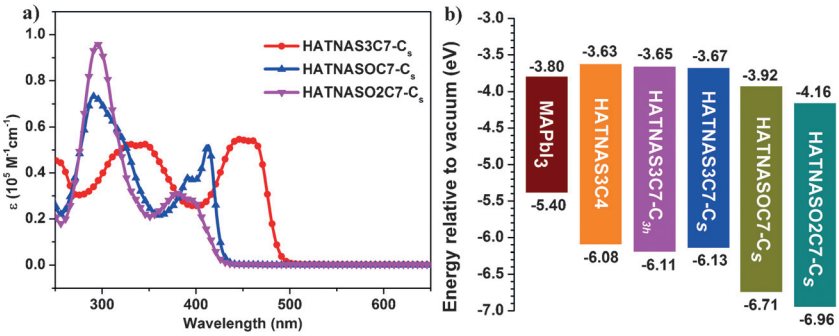

Figure 2. a) UV/Vis absorption spectra of HATNAS3C7-C_s, HATNASOC7-C_s, and HATNASO2C7-C_s in $CHCl_3$ (concentration = 1×10^{-5} M, at room temperature) showing molar extinction coefficients (ε). b) Corresponding energy levels of the HATNA derivatives.

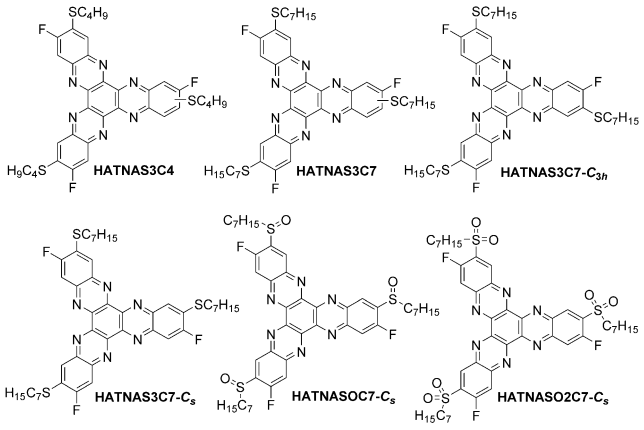

Scheme 1. Chemical structures of HATNA-derived ETMs for PVSCs.

energetically lower than that of the CBM of $MAPbI_3$, which facilitates electron transport (Figure 2b). Notably, although the LUMOs of the alkylsulfanyl-substituted HATNA derivatives are slightly higher than that of the perovskite film CBM, their significantly deeper HOMO than the valence band maximum (VBM) of perovskite induced better performance due to efficient hole blocking to prevent charge recombination at the corresponding interfaces (Figure 2b).

To evaluate the function of these HATNA derivatives as ETMs, PVSCs with an inverted p–i–n planar-heterojunction (PHJ) architecture of ITO/NiO_x (≈30 nm)/$MAPbI_3$ (≈350 nm)/ETM (≈80 nm)/Ag were fabricated (ITO = indium tin oxide). The cross-sectional scanning electron microscopy (SEM) image of the device is displayed in Figure 3a. The performance of the studied PVSC is summarized in Table 1 and the *J–V* curves are shown in Figure 3b. The external quantum efficiency (EQE) spectra of these PVSCs are also measured (Figure S5), in which the integrated short-circuit current (J_{SC}) is consistent with the measured values. A control device based on a PCBM ETM yielded an optimal PCE of 15.91%, which is similar to the performance reported for a similar device structure and processing conditions.[13] By replacing PCBM with HATNA-F_6, the performance of device significantly decreased because the very poor solubility of HATNA-F_6 means that homogeneous thin films cannot be obtained (Figure S6). By switching from HATNA-F_6 to alkylsulfanyl-substituted HATNA derivatives (HATNAS3C4, HATNAS3C7, HATNAS3C7-C_{3h}, and HATNAS3C7-C_s), improved performance could be achieved in all cases, which might be due to their better solubility and hole-blocking properties. We noticed that both the J_{sc} value and the fill factor (FF) can be improved when the length of the side-chain was increased for alkylsulfanyl-substituted HATNA derivatives (HATNAS3C4 versus HATNAS3C7; Table 1). This effect might be attributable to an enhanced processability and a higher electron mobility.[11]

Table 1: Summary of photovoltaic parameters derived from *J–V* measurements of perovskite solar cells.

ETMs	V_{oc} [V]	J_{sc} [mA cm^{-2}]	FF [%]	PCE [%]	μ_e[a] [cm^2 V^{-1} s^{-1}]
PCBM	1.06	19.59	76.5	15.91	3.92×10^{-3}
HATNA-F_6	0.85	10.17	57.6	4.69	–
HATNAS3C4	0.95	16.81	72.8	11.59	0.83×10^{-3}
HATNAS3C7	0.95	18.28	76.1	13.49	1.45×10^{-3}
HATNAS3C7-C_{3h}	0.96	18.31	76.3	13.38	1.58×10^{-3}
HATNAS3C7-C_s	0.94	19.69	75.8	13.95	1.36×10^{-3}
HATNASOC7-C_s	1.08	20.73	78.6	17.62	5.13×10^{-3}
HATNASO2C7-C_s	1.00	19.44	74.2	14.42	2.34×10^{-3}

[a] The electron transport of the HATNA derivatives was measured by using the SCLC technique (see Figure S7).

All of the alkylsulfanyl-substituted HATNA-derived devices exhibited a similar J_{sc} value but a lower open-circuit voltage (V_{oc}) compared with the device based on PCBM because of the higher LUMO level of these derivatives than the CBM of the perovskite film. It should also be noted that similar PCE performances were recorded for the three compounds HATNAS3C7 (PCE = 13.49%), HATNAS3C7-C_{3h} (PCE = 13.38%), and HATNAS3C7-C_s (PCE = 13.95%), indicating that symmetry does not determine photovoltaic performance. Further study demonstrated that a superior performance can be achieved when the ETM was changed to HATNASOC7-C_s (Table 1). The observed PCE (17.62%) outperforms that of the control device using PCBM as the ETM (PCE = 15.91%). However, switching the ETM to HATNASO2C7-C_s only led to moderate device performance (PCE = 14.42%). This disimprovement may be as a result of the lower electron mobility of the molecule and the fact that it is less planar than HATNASO2C7-C_s, as well as the bigger energy offset between the LUMO of the molecule and the CBM of $MAPbI_3$.

To investigate the current hysteresis for our devices,[14] the HATNASOC7-C_s based device was examined in both the forward scan and the reverse scan directions. As shown in Figure 3c, the reverse scan yielded a high PCE of 17.62%, and the forward scan only showed a slightly different PCE of 17.22%. Furthermore, the *J–V* curves at various scanning rates only showed negligible differences for our HATNASOC7-C_s based device (Figure S8). More importantly, the PCE in HATNASOC7-C_s based devices exhibited

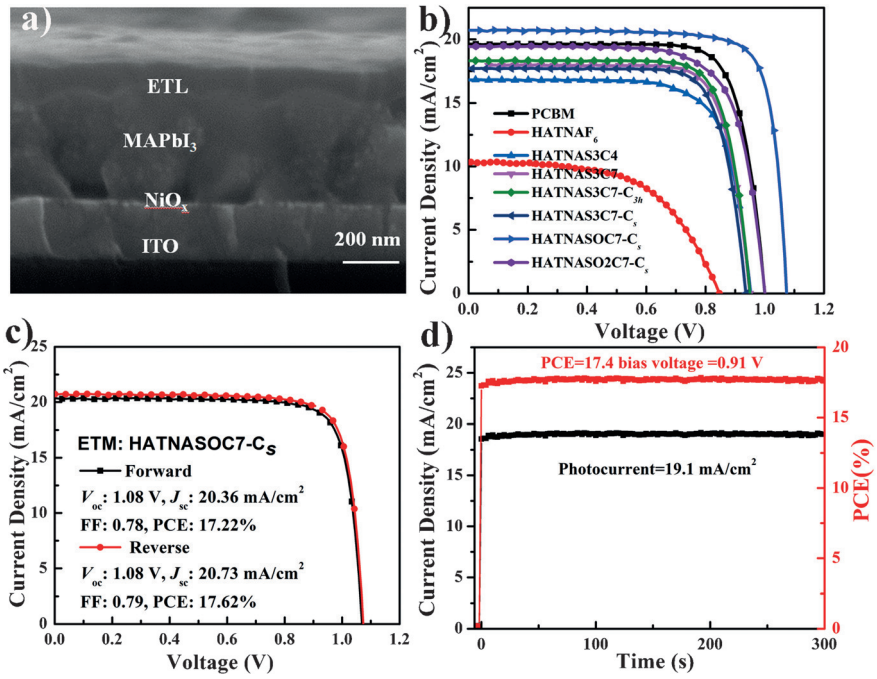

Figure 3. a) Cross-section SEM image of the cell architecture; b) *J–V* curves of the best performing PVSCs prepared with ETMs; c) *J–V* curve of HATNASOC7-C_s showing both the forward scan and the reverse scan; d) stabilized photocurrent measurement of the best device incorporating HATNASOC7-C_s as the ETM and its power output.

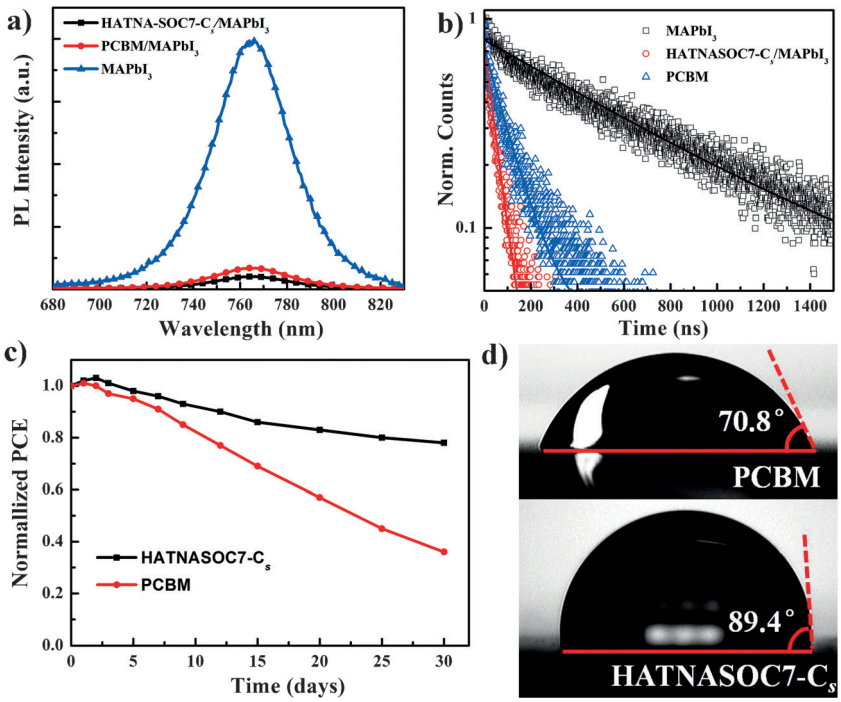

Figure 4. a) Steady-state PL spectra of the perovskite films on different substrates; b) time-resolved PL measurements taken at the emission wavelength ($\lambda = 765$ nm) of the perovskite films on different substrates; c) stability test of the PVSCs in ambient air with a controlled humidity of about 40–50%; d) water contact angles on HATNASOC7-C_s and PCBM film.

excellent reproducibility, with 80% of the measured devices showed PCE values of over 16% (Figure S9). In addition, the photocurrent density and PCE as a function of time were measured at 0.91 V (near the maximum power point, Figure 2d and Figure S10). As shown, a steady-state PCE of about 17.4% with a J_{SC} value of 19.1 mA cm^{-2} could be clearly observed, confirming the reliable high performance. This evidence clearly showed that no apparent current hysteresis was induced during forward and reverse scans.

To understand the interactions between HATNASOC7-C_s and $MAPbI_3$ and to explain the performance differences between HATNASOC7-C_s and PCBM as ETMs, steady-state photoluminescence (PL) and time-resolved PL decay measurements were conducted for neat-film perovskites with a layer of HATNASOC7-C_s or PCBM as shown in Figure 4a,b. Notably, HATNASOC7-C_s showed a slightly higher PL quenching efficiency than PCBM, suggesting more efficient electron extraction from perovksite to HATNASOC7-C_s. This result is in accordance with the higher space-charge-limited current (SCLC) electron mobility (μ_e) measured for HATNASOC7-C_s than PCBM (Table 1). The time-resolved PL measurements further verified the improved electron transfer when HATNASOC7-C_s was used as the ETM (Figure 4b and Table S2). Compared to the perovskite-only film with a decay time (τ) of 676.5 ns,[15] the introduction of HATNASOC7-C_s or PCBM on top of $MAPbI_3$ significantly shortened the PL decay time to 46.9 ns and 102.8 ns, respectively. The shortened decay lifetime of perovskite with HATNASOC7-C_s provided further evidence for the more efficient electron extraction and charge dissociation from perovskite to HATNASOC7-C_s.

The employment of HATNA derivatives as the ETM also significantly enhanced the stability of PVSCs. As shown in Figure 4c, the PVSC with HATNASOC7-C_s as the ETM can retain more than 80% of its original PCE value after being stored in air for 30 days without encapsulation. In contrast, the PCBM-based device lost almost 70% of its original PCE value after the same period of time. To explain this improvement, the contact angles of water droplets on HATNASOC7-C_s and PCBM were measured. As shown in Figure 4d, HATNASOC7-C_s exhibit a contact angle of about 89.4°, whereas the angle was only 70.8° for PCBM. Thus, the better hydrophobicity of HATNASOC7-C_s may help improve the long-term stability of the devices. The improved stability may also be due to the passivation of the perovskite surface traps by the coordination between sulfoxide (S=O) and Pb, which has been reported by Choi, Park, and co-workers.[16]

In summary, a series of HATNA derivatives peripherally functionalized with alkylsulfanyl chains of different lengths and with different sulfur oxidation states (sulfide, sulfoxide, and sulfone) were prepared in order to improve the solution processability of the compounds and well as to fine tune their energy levels. The resultant HATNA derivatives can function as efficient ETMs, with the PVSCs prepared incorporating the compounds having superior PCE values (up to 17.6%) with negligible hysteresis. HATNASOC7-C_s is one of the first nonfullerene small-molecule ETMs which can be used to obtain a high-performance p–i–n PVSC. The PCE value reported here is among the highest reported for inverted PVSCs using nonfullerene ETMs. These new nonfullerene ETMs can potentially be used to replace fullerenes in inverted PVSCs. Moreover, these hydrophobic ETMs and their potential ability to passivate the surface traps of perovskites endow the resulting PVSCs with significantly improved device stability.

Acknowledgements

This work was supported by the Office of Naval Research (N00014-14-1-0246), the Asian Office of Aerospace R&D (FA2386-15-1-4106), and the Department of Energy SunShot (DEEE0006710). A.K.-Y.J. thanks the Boeing-Johnson Foundation for financial support.

Keywords: electron-transporting materials · energy conversion · perovskite phases · photovoltaics · solar cells

How to cite: *Angew. Chem. Int. Ed.* **2016**, *55*, 8999–9003
Angew. Chem. **2016**, *128*, 9145–9149

[1] For recent reviews on PVSCs, see: a) H. J. Snaith, *J. Phys. Chem. Lett.* **2013**, *4*, 3623; b) N.-G. Park, *J. Phys. Chem. Lett.* **2013**, *4*, 2423; c) M. A. Green, A. Ho-Baillie, H. J. Snaith, *Nat. Photonics* **2014**, *8*, 506; d) S. T. Williams, A. Rajagopal, C.-C. Chueh, A. K. Y. Jen, *J. Phys. Chem. Lett.* **2016**, *7*, 811; e) A. R. b. M. Yusoff, M. K. Nazeeruddin, *J. Phys. Chem. Lett.* **2016**, *7*, 851; f) A. Sharenko, M. F. Toney, *J. Am. Chem. Soc.* **2016**, *138*, 463.

[2] For some reviews, see: a) J. Shi, X. Xu, D. Li, Q. Meng, *Small* **2015**, *11*, 2472; b) C.-C. Chueh, C.-Z. Li, A. K. Y. Jen, *Energy Environ. Sci.* **2015**, *8*, 1160. For some recent examples, see: c) L. Liu, A. Mei, T. Liu, P. Jiang, Y. Sheng, L. Zhang, H. Han, *J. Am. Chem. Soc.* **2015**, *137*, 1790; d) L. Zuo, Z. Gu, T. Ye, W. Fu, G. Wu, H. Li, H. Chen, *J. Am. Chem. Soc.* **2015**, *137*, 2674; e) C. Kuang, G. Tang, T. Jiu, H. Yang, H. Liu, B. Li, W. Luo, X. Li, W. Zhang, F. Lu, J. Fang, Y. Li, *Nano Lett.* **2015**, *15*, 2756; f) H. Azimi, T. Ameri, H. Zhang, Y. Hou, C. O. R. Quiroz, J. Min, M. Hu, Z.-G. Zhang, T. Przybilla, G. J. Matt, E. Spiecker, Y. Li, C. J. Brabec, *Adv. Energy Mater.* **2015**, *5*, 1401692; g) Y. Li, Y. Zhao, Q. Chen, Y. Yang, Y. Liu, Z. Hong, Z. Liu, Y.-T. Hsieh, L. Meng, Y. Li, Y. Yang, *J. Am. Chem. Soc.* **2015**, *137*, 15540.

[3] For some reviews on HTMs for PVSCs, see: a) S. Ameen, M. A. Rub, S. A. Kosa, K. A. Alamry, M. S. Akhtar, H.-S. Shin, H.-K. Seo, A. M. Asiri, M. K. Nazeeruddin, *ChemSusChem* **2016**, *9*, 10; b) S. F. Völker, S. Collavini, J. L. Delgado, *ChemSusChem* **2015**, *8*, 3012.

[4] For a very recent review, see: M. Ye, X. Hong, F. Zhang, X. Liu, *J. Mater. Chem. A* **2016**, *4*, 6755.

[5] For some examples using fullerene derivatives as ETMs for PVSCs, see: a) J.-Y. Jeng, Y.-F. Chiang, M.-H. Lee, S.-R. Peng, T.-F. Guo, P. Chen, T.-C. Wen, *Adv. Mater.* **2013**, *25*, 3727; b) O. Malinkiewicz, A. Yella, Y. H. Lee, G. M. Espallargas, M. Graetzel, M. K. Nazeeruddin, H. J. Bolink, *Nat. Photonics* **2014**, *8*, 128; c) Z. Zhu, Y. Bai, T. Zhang, Z. Liu, X. Long, Z. Wei, Z. Wang, L. Zhang, J. Wang, F. Yan, S. Yang, *Angew. Chem. Int. Ed.* **2014**, *53*, 12571; *Angew. Chem.* **2014**, *126*, 12779; d) P.-W. Liang, C.-C. Chueh, S. T. Williams, A. K. Y. Jen, *Adv. Energy Mater.* **2015**, *5*, 1402321; e) J. H. Kim, C.-C. Chueh, S. T. Williams, A. K. Y. Jen, *Nanoscale* **2015**, *7*, 17343; f) S. Collavini, I. Kosta, S. F. Vçlker, G. Cabanero, H. J. Grande, R. Tena-Zaera,J. L. Delgado, *ChemSusChem* **2016**, DOI: 10.1002/cssc.201600051.

[6] Recently, n-type polymers and ZnO nanoparticles were used as ETMs for *p*-i-n PVSCs (relatively low PCE with apparent current hysteresis was achieved in some cases). See: a) C. Sun, Z. Wu, H.-L. Yip, H. Zhang, X.-F. Jiang, Q. Xue, Z. Hu, Z. Hu, Y. Shen, M. Wang, F. Huang, Y. Cao, *Adv. Energy Mater.* **2015**, 1501534; b) W. Wang, J. Yuan, G. Shi, X. Zhu, S. Shi, Z. Liu, L. Han, H.-Q. Wang, W. Ma, *ACS Appl. Mater. Interfaces* **2015**, *7*, 3994; c) S. Shao, Z. Chen, H.-H. Fang, G. H. ten Brink, D. Bartesaghi, S. Adjokatse, L. J. A. Koster, B. J. Kooi, A. Facchetti, M. A. Loi, *J. Mater. Chem. A* **2016**, *4*, 2419; d) J. You, L. Meng, T.-B. Song, T.-F. Guo, Y. Yang, W.-H. Chang, Z. Hong, H. Chen, H. Zhou, Q. Chen, Y. Liu, N. D. Marco, Y. Yang, *Nat. Nanotechnol.* **2016**, *11*, 75.

[7] a) C. J. Brabec, A. Cravino, D. Meissner, N. S. Sariciftci, T. Fromherz, M. T. Rispens, L. Sanchez, J. C. Hummelen, *Adv. Funct. Mater.* **2001**, *11*, 374; b) Y. He, H.-Y. Chen, J. Hou, Y. Li, *J. Am. Chem. Soc.* **2010**, *132*, 1377; c) A. Anctil, C. W. Babbitt, R. P. Raffaelle, B. J. Landi, *Environ. Sci. Technol.* **2011**, *45*, 2353.

[8] Two nonfullerene small organic molecules have been investigated as ETMs for PVSCs but have yielded only very poor performances (PCE < 8%). See: a) O. Malinkiewicz, C. Roldán-Carmona, A. Soriano, E. Bandiello, L. Camacho, M. K. Nazeeruddin, H. J. Bolink, *Adv. Energy Mater.* **2014**, *4*, 1400345; b) J. Huang, Z. Gu, L. Zuo, T. Ye, H. Chen, *Solar Energy* **2016**, *133*, 331.

[9] a) H. Bock, A. Babeau, I. Seguy, P. Jolinat, P. Destruel, *ChemPhysChem* **2002**, *3*, 532; b) C. W. Ong, S. C. Liao, T. H. Chang, H. F. Hsu, *J. Org. Chem.* **2004**, *69*, 3181; c) B. R. Kaafarani, T. Kondo, J. S. Yu, Q. Zhang, D. Dattilo, C. Risko, S. C. Jones, S. Barlow, B. Domercq, F. Amy, A. Kahn, J. L. Bredas, B. Kippelen, S. R. Marder, *J. Am. Chem. Soc.* **2005**, *127*, 16358; d) S. Furukawa, T. Okubo, S. Masaoka, D. Tanaka, H. C. Chang, S. Kitagawa, *Angew. Chem. Int. Ed.* **2005**, *44*, 2700; *Angew. Chem.* **2005**, *117*, 2760; e) T. Ishi-i, K. Yaguma, R. Kuwahara, Y. Taguri, S. Mataka, *Org. Lett.* **2006**, *8*, 585; f) H. L. Yip, J. Zou, H. Ma, Y. Tian, N. M. Tucker, A. K. Y. Jen, *J. Am. Chem. Soc.* **2006**, *128*, 13042; g) S. D. Ha, B. R. Kaafarani, S. Barlow, S. R. Marder, A. Kahn, *J. Phys. Chem. C* **2007**, *111*, 10493; h) S. Choudhary, C. Gozalvez, A. Higelin, I. Krossing, M. Melle-Franco, A. Mateo-Alonso, *Chem. Eur. J.* **2014**, *20*, 1525; i) X.-Y. Liu, T. Usui, J. Hanna, *Chem. Eur. J.* **2014**, *20*, 14207.

[10] a) S. Barlow, Q. Zhang, B. R. Kaafarani, C. Risko, F. Amy, C. K. Chan, S. R. Marder, *Chem. Eur. J.* **2007**, *13*, 3537; b) F. Selzer, C. Falkenberg, M. Hamburger, M. Baumgarten, K. Müllen, K. Leo, M. Riede, *J. Appl. Phys.* **2014**, *115*, 054515.

[11] M. Lehmann, G. Kestemont, R. G. Aspe, C. Buess-Herman, M. H. J. Koch, M. G. Debije, J. Piris, M. P. de Haas, J. M. Warman, M. D. Watson, V. Lemaur, J. Cornil, Y. H. Geerts, R. Gearba, D. A. Ivanov, *Chem. Eur. J.* **2005**, *11*, 3349.

[12] a) N. K. Noel, A. Abate, S. D. Stranks, E. S. Parrott, V. M. Burlakov, A. Goriely, H. J. Snaith, *ACS Nano* **2014**, *8*, 9815; b) J. Cao, J. Yin, S. Yuan, Y. Zhao, J. Li, N. Zheng, *Nanoscale* **2015**, *7*, 9443; c) J. Cao, Y.-M. Liu, X. Jing, J. Yin, J. Li, B. Xu, Y.-Z. Tan, *J. Am. Chem. Soc.* **2015**, *137*, 10914.

[13] a) J. H. Kim, P.-W. Liang, S. T. Williams, N. Cho, C.-C. Chueh, M. S. Glaz, D. S. Ginger, A. K. Y. Jen, *Adv. Mater.* **2015**, *27*, 695; b) J. W. Jung, C.-C. Chueh, A. K. Y. Jen, *Adv. Mater.* **2015**, *27*, 7874; c) Z. Yang, C.-C. Chueh, P.-W. Liang, M. Crump, F, Lin, Z. Zhu, A. K. Y. Jen, *Nano Energy* **2016**, *22*, 328.

[14] a) M. Grätzel, *Nat. Mater.* **2014**, *13*, 838; b) H. J. Snaith, A. Abate, J. M. Ball, G. E. Eperon, T. Leijtens, N. K. Noel, S. D. Stranks, J. T.-W. Wang, K. Wojciechowski, W. Zhang, *J. Phys. Chem. Lett.* **2014**, *5*, 1511; c) T. Leijtens, G. E. Eperon, N. K. Noel, S. N. Habisreutinger, A. Petrozza, H. J. Snaith, *Adv. Energy Mater.* **2015**, *5*, 1500963.

[15] The lifetime is in accordance with the previous report by Snaith and co-workers: S. D. Stranks, G. E. Eperon, G. Grancini, C. Menelaou, M. J. P. Alcocer, T. Leijtens, L. M. Herz, A. Petrozza, H. J. Snaith, *Science* **2013**, *342*, 341.

[16] N. Ahn, D.-Y. Son, I.-H. Jang, S. M. Kang, M. Choi, N.-G. Park, *J. Am. Chem. Soc.* **2015**, *137*, 8696.

Received: May 5, 2016
Published online: June 8, 2016

